# Kinetics of Surface-Initiated Atom Transfer Radical Polymerization of Acrylamide on Silica

**Deqing Xiao and Mary J. Wirth***

*Department of Chemistry, University of Delaware, Newark, Delaware 19716*

*Received July 23, 2001*

ABSTRACT: Surface-initiated atom transfer radical polymerization (ATRP) of acrylamide is achieved on silica at room temperature by using a catalytic system of $CuCl/CuCl_2$/tris(2-dimethylaminoethyl)-amine. The thickness of the polyacrylamide film is proportional to the monomer concentration but not to reaction time. This behavior is qualitatively similar to that for surface ATRP of acrylamide using a CuCl/bipyridine catalytic system, which required 130 °C for initiation. A kinetic study shows that, at room temperature, both the rate for chain propagation and the rate of chain termination are higher, despite a much higher concentration of Cu(II) to reduce the radical population at room temperature. XPS shows that the concentration of chlorine at the surface drops as the polymerization reaction progresses, indicating that termination is caused by radical combination. For polymerization on silica gel at room temperature, microanalysis shows that half of the chlorine is lost during polymerization. Equilibration of the surface-bound initiator with only the copper catalyst shows that most of the chlorine loss is due to the combination of initiator radicals.

## Introduction

Recently, controlled free radical polymerization techniques have been used to synthesize polymers with narrow polydispersities and predetermined molecular weights.[1−5] The application of these techniques opened new ways for the modification of solid substrates for their potential applications in a variety of technological fields. Polymer films with thicknesses in molecular dimensions attached to solid substrates are very versatile in bringing the surface new properties.[6] Compared with traditional physisorption,[7] "grafting to",[8] and "grafting from" methods,[9] the advantage of controlled free radical polymerization techniques is their tailoring potential in that the film thickness is adjustable; the film properties can be finely tuned by introducing varieties of functional groups or by copolymerization and polymer patterning by the microcontact technique.[10]

All three controlled free radical polymerization methods, namely the atom transfer radical polymerization (ATRP),[11−15] the nitroxide-mediated free radical polymerization (TEMPO),[16−18] and the polymerization method based on iniferters,[19] have been applied to grow polymer films on the surface of a substrate by grafting the initiator directly to the surface.[20−26] While the method of iniferters is plagued by high polydispersities and poor control over the functional groups at the chain ends[27] and the method of TEMPO is mainly used in the research of the polymerization or copolymerization of styrene and its derivatives, ATRP appears to be the most versatile[28] for preparing polystyrene(s),[12,14,29−31] poly(methyl methacrylate) (PMMA),[32−34] polyacrylate,[35] poly(methyl acrylate),[36] and their copolymers,[37−39] with well-controlled molecular weight and well-defined structures. In a typical ATRP reaction, CuCl or CuBr is generally used as catalyst and bipyridines or multidentitate amines as the ligand. The range of reaction temperatures is 100−130 °C. For catalytic initiation by chlorinated derivatives, a rather high temperature of 130 °C is necessary, which might cause side reactions.

* Corresponding author.

There are several factors that can affect the reaction temperature, namely the catalyst, the monomer, the solvent, and the ligand that complexes with the catalyst. The ligand has been reported to be an especially strong factor in the reaction temperature. The ligand must have a high complexation constant to compete with the polyacrylamide for copper, and it must allow fast redox between Cu(I) and Cu(II). A multidentate amine, (PMDETA), allows initiation at 110 °C, but polymerization is slow and uncontrolled.[40] In the case of solution polymerization of (meth)acrylamide, it has been reported that tris[2-(dimethylamino)ethyl] amine ($Me_6$-TREN) forms a complex with Cu(I) that is more reducing and powerful.[41] The reason is the quadridentate tripodal nitrogen donor ligand $Me_6$TREN forms high spin, five coordinated complexes with copper(II) of the type[M($Me_6$TREN)X]X, which have a trigonal bipyramidal structure,[42] enabling the easy valence change of copper. With this ligand, solution polymerizations of *N*,*N*-dimethylacrylamide, *N*-*tert*-butylacrylamide, and *N*-(2-hydroxypropyl)methacrylamide were achieved in a controlled manner at room temperature.[41]

The ability to initiate ATRP at room temperature offers advantages for the growth of chains on surfaces. The most significant advantage is that thermally formed polymer, which can foul the surface or clog nanoscale pores, is avoided by operation at room temperature. In our previous papers,[23−25] we reported for the polymerization of acrylamide at 130 °C that the polymer chains grow proportionally to the monomer concentration. However, when we observed the chain length dependence on time, we did not find a linear relationship.[43] Instead, the polymer growth leveled off after about 10 h. It was assumed that the termination was related to thermal polymerization because the solution became more viscous. The behavior was not studied further. The advent of radical polymerization at room-temperature now makes the nature of termination interesting because thermal polymerization can be eliminated. Other mechanisms for termination are possible, as well. As one possibility, for any radical polymerization, radical

10.1021/ma011313x CCC: $22.00 
Published on Web 03/07/2002

transfer can occur from the intended, surface-bound radical to an acrylamide monomer in solution. The possibility has been suggested that nucleophilic displacement of the terminal chlorine by $-NH_2$ can occur to form a heterocycle, yielding an amino chloride functionality.[40] A third possibility that the Cu(II) species in the solution can act as the catalyst for the extraction of HX in atom-transfer living polymerization.[44] Each of these termination reactions is first order with respect to radical concentration. Additionally, since surface-bound radicals can, in principle, be generated at high concentrations due to the proximity of adjacent initiators, radical annihilation could occur. This process would be second order in radical concentration. Characterizing termination is important to the control of the growth of polymer chains from surfaces. The purpose of this paper is to investigate the kinetics of ATRP for the growth of polyacrylamide on silica surfaces.

## Experimental Section

**Materials and Equipment.** Acrylamide (electrophoresis grade, 99.9%) was obtained from Fisher Scientific. CuCl (99+%) was obtained from Aldrich and was purified according to the published procedure.[15] $CuCl_2$ (anhydrous, 99+%) was obtained from Acros and used as received. Formic acid (reagent grade ACS 88+%) and tris(2-aminoethyl)amine(TREN, 96%) were obtained from Acros. Tris[2-(dimethylamino)ethyl]amine-($Me_6$TREN) was prepared from TREN by a procedure similar to that of Ciampolini and Nardi[45] and stored under argon. 1-Trichlorosilyl-2-*m*-*p*-chloromethyl phenyl)ethane was obtained from United Chemical Technology, Inc. Silica gel (Nucleosil 1000 Å S-5 $\mu$m) was obtained from The Nest Group, Inc. Silica gel (Nucleosil 300 Å S-5 $\mu$m) was obtained from Phenomenex. Silicon wafers (3 in. diameter, 20.5−21.5 mm thickness, orientation 100, both sides polished) were obtained from Semicondutor Processing Co. (Boston, MA). The fused-silica coverslips were obtained from Esco Products. All other solvents (reagent or HPLC grade) were from Fisher Chemicals. The proteins used were from Sigma.

**Preparation of Benzyl Chloride Monolayer on Silicon Wafers.** The silicon wafer disk was cut into small pieces (2.5 cm × 2.5 cm) before cleaning. The small pieces of wafer were boiled in $HNO_3$:$H_2O$ (50:50, V:V) for 4.0 h and then rinsed with a copious amount of pure water. The cleaned wafers were dried at 120 °C in an oven for 2.0 h. Then the dried wafers were placed into a 500 mL flask (specially made so the wafers can be separated in the flask) and humidified at 50% relative humidity briefly. Then 1 mL of 1-trichlorosily-2-(*m*-*p*-chloromethyl phenyl) ethane was added to 100 mL of toluene which was dried by passing through an $Al_2O_3$:$SiO_2$ packed column. The above solution was sonicated for 30 s and then immediately added to the flask containing the silicon wafers. The flask was purged with nitrogen for the first 5 min of the reaction as HCl evolved and then sealed with the stopper. The reaction proceeded at room-temperature overnight. After the reaction, the wafers were rinsed with toluene and acetone and dried in an oven at 110 °C for 1.0 h.

**Preparation of Benzyl Chloride Monolayer on Silica Gel.** The silica gel was first cleaned in $HNO_3$:$H_2O$ (50:50, V:V) for 4 h, rinsed with large amounts of distilled water, and dried under nitrogen in a tube furnace for 3 h. Then 3.0 g of the above silica gel was humidified at 50% relative humidity for 4 h and placed in a 250 mL flask, and 0.35 mL of 1-trichlorosilyl-2-(*m*,*p*-chloromethyl phenyl) ethane was added to 60 mL of dried toluene. This solution was immediately added to the reaction flask. The flask was purged with nitrogen for the first 5 min of the reaction as HCl evolved, and then sealed with the stopper. The reaction proceeded at room-temperature overnight. After the reaction, the silica gel was filtered and rinsed with toluene, methanol, methylene chloride and acetone and dried in an oven at 110 °C for 1.0 h.

**Surface ATRP of Acrylamide on Silicon Wafer or Silica Gel.** A typical procedure for reactions using a CuCl/bipyridine catalytic system at 130 °C was mentioned in our previous papers.[23−25] A typical procedure for reactions using a CuCl/$CuCl_2$/$Me_6$TREN catalytic system at room temperature is as follows: A Schlenk flask was charged with 49.5 mg (500 $\mu$mol) of CuCl, 6.7 mg (50 $\mu$mol) of $CuCl_2$, and silicon wafers or silica gel. The flask was sealed with a rubber stopper and cycled between vacuum and argon three times to remove oxygen. A 20 mL solution of 3 M acrylamide in DMF was bubbled with argon for 45 min and then transferred into the flask via a syringe. After the catalyst has completely dissolved 0.17 mL (600 $\mu$mol) of $Me_6$TREN was injected into the flask. The reaction solution was then transferred to another flask containing silicon wafers, or 0.5 g of silica gel, which was sealed with a rubber stopper and cycled between vacuum and argon at least three times to remove oxygen. Then the flask was placed in a water bath at room temperature. The thickness of the polyacrylamide film was determined from the infrared absorbance of the C=O stretch. A linear calibration curve of thickness and absorbance was used to convert the absorbance to the thickness.[19]

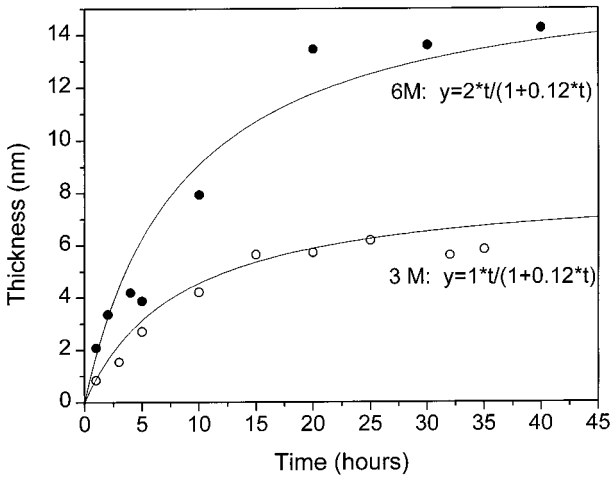


**Figure 1.** Thickness of polyacrylamide film vs time for ATRP on silicon wafers at 130 °C. Two different acrylamide concentrations were used: 6 and 3 M. The data are indicated by the points and the curves show the best fit to eq 5.

**X-ray Photoelectron Spectroscopy.** XPS was performed on a SSI 310 *x*-probe spectrometer using Al Kα radiation at 1487 eV to determine the surface composition of the substrates with organic layer.

**$^{13}$C Solid State NMR Spectroscopy.** Solid -state NMR spectroscopy was completed using a Bruker MSL 300 spectrometer. Single-pulse excitation was used along with proton decoupling. Single-pulse excitation was shown to be sensitive to the molecular motion of the groups on the unbound end of the alkyl chains and proton decoupling reduced influences associated with heteronuclear dipolar coupling. The sample was spun at a rate of 3000 Hz at the magic angle to remove line-broadening influences due to chemical-shift anisotropy.[46,47]

## Result and Discussion

We previously showed that the thickness of living polyacrylamide on silica surfaces, grown at 130 °C using bipyridine as the catalyst, was linear in monomer concentration,[25] but we had preliminary evidence that thickness was not linear in time.[43] To investigate this behavior in more detail, we have chosen two monomer concentrations and studied the growth as a function of time on a silicon wafer. Figure 1 shows the polyacrylamide thickness vs time, where monomer concentrations of 3 and 6 M are used. In both cases, the film thickness levels off as the reaction proceeds. The limiting surface concentration is proportional to monomer concentration within experimental error, which is largely due to the error in the infrared spectral intensities. While the

**Scheme 1**

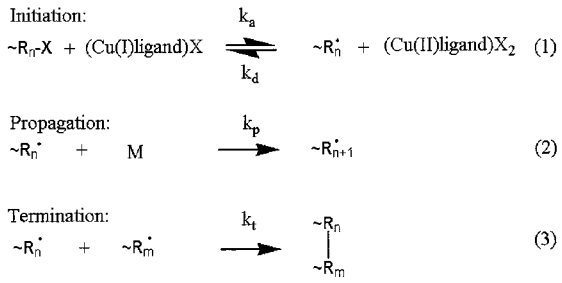


linearity in monomer concentration ostensibly suggests living polymerization, the nonlinearity in the time dependence indicates termination. We have observed that the solution always becomes increasingly viscous with time, indicating solution polymerization occurs. The roll-off in thickness could be due to the solution polymer causing either a drop in monomer concentration or the fouling of the surface by polymer in solution. The roll-off in thickness could also be due to termination from radical combination. To explain how the growth of the polymer could be linear in monomer concentration, despite termination, requires a testable model.

The initiation and propagation steps of living radical polymerization can be written as shown in Scheme 1.

Monomer disappears only due to propagation, step 2 of Scheme 1.

$$-\frac{\mathrm{d}[\mathrm{M}]}{\mathrm{d}t} = k_\mathrm{p}[\sim\mathrm{R}^\bullet][\mathrm{M}] \qquad (1)$$

If [~R•] is constant, the monomer concentration is reduced in accord with first-order kinetics.

$$\frac{[\mathrm{M}]}{[\mathrm{M}]_0} = \exp(-k_\mathrm{p}[\sim\mathrm{R}^\bullet]t) \qquad (2)$$

However, [~R•] is not necessarily constant. Fischer[48] derived a rate expression for the radical by considering the first and third reactions in Scheme 1.

$$\frac{\mathrm{d}[R^\bullet]}{\mathrm{d}t} = k_\mathrm{a}[\sim\mathrm{R{-}X}] - k_\mathrm{d}[\sim\mathrm{R}^\bullet] - k_\mathrm{t}[\sim\mathrm{R}^\bullet]^2 \qquad (3)$$

The expression for the equilibrium constant helps to illustrate the conditions under which equilibrium can be approached.

$$K_\mathrm{eq} = \frac{k_\mathrm{a}}{k_\mathrm{d}} = \frac{[\sim\mathrm{R}^\bullet][\mathrm{Cu^{II}LX_2}]}{[\sim\mathrm{R{-}X}][\mathrm{Cu^{I}LX}]} \qquad (4)$$

In Fischer's detailed treatment,[48] equilibrium is maintained but Cu(II) accumulates over time due to combination of radicals. The accumulating Cu(II) suppresses termination, and this time dependence complicates the time dependence of [~R•]. Fischer derived an expression to show that [~R•] depends on $t^{1/3}$ and that conversion, $p$, has a $t^{2/3}$ dependence.

$$p = 1 - \frac{[\mathrm{M}]}{[\mathrm{M}]_0} = 1 - \exp\left(-\frac{3}{2}k_\mathrm{p}\left(\frac{k_\mathrm{a}[\sim\mathrm{R{-}X}]_0[\mathrm{Cu(I)}]_0}{3k_\mathrm{t}}\right)^{1/3} t^{2/3}\right) \qquad (5)$$

To apply Fischer's model to the system at hand, which entails polymer chains growing from a surface, thickness is proportional to $p[\mathrm{M}]_0$. It is noted here that we do not typically report conversion for surface polymerization because $p \approx 10^{-4}$ for the reaction of monomer to initiators on flat surfaces. In solution polymerization, high conversion is valuable. In surface polymerization, high surface coverage is valuable, not conversion. Equation 5 shows, for a given reaction time, the thickness is proportional to the initial monomer concentration regardless of the complicated time dependence or radical combination. Hence, our observation that film thickness is proportional to monomer concentration says nothing about the extent of radical combination, i.e., about whether the reaction approaches living polymerization. A kinetic analysis is required to judge the importance of radical combination.

It is evident that the model of Fischer[48] does not apply because eq 5 predicts that complete conversion is approached at infinite time, yet experimentally the surface reaction appears to be stopped at these miniscule conversions. Fischer's elegant model is valuable for solution polymerization but does not apply for polymerization to low surface area materials because there are so few moles of initiator relative to molecules of catalyst that the initiation is not a significant source of Cu(II). The Cu(II) does not accumulate significantly to suppress termination, and a different model is required.

Since the concentration of Cu(II) does not significantly change for a material with few moles of initiator, [~R•] changes only due to termination. This neglects possible contributions from surface fouling or side reactions, such as radical transfer to solution.

$$\frac{\mathrm{d}[\sim\mathrm{R}^\bullet]}{\mathrm{d}t} = -k_\mathrm{t}[\sim\mathrm{R}^\bullet]^2 \qquad (6)$$

$$[\sim\mathrm{R}^\bullet] = \left(\frac{[\sim\mathrm{R}^\bullet]_0}{1 + [\sim\mathrm{R}^\bullet]_0 k_\mathrm{t} t}\right) \qquad (7)$$

Recognizing that monomer concentration changes negligibly for so few moles of initiator, this simplifies the solution of eq 2.

$$\frac{[\mathrm{M}]}{[\mathrm{M}]_0} \approx 1 - k_\mathrm{p}[\sim\mathrm{R}^\bullet]t \qquad (8)$$

By substitution of eq 7 into eq 8, the conversion would have a simple nonlinear time dependence when termination occurs.

$$[\mathrm{M}]_0 - [\mathrm{M}] = \frac{[\mathrm{M}]_0 k_\mathrm{p}[\sim\mathrm{R}^\bullet]_0 t}{1 + [\sim\mathrm{R}^\bullet]_0 k_\mathrm{t} t} \qquad (9)$$

Recognizing that ellipsometric thickness is proportional to $[\mathrm{M}]_0 - [\mathrm{M}]$, the data of Figure 1 are fit to eq 9, and the solid lines show that the quality of the fit is good at both concentrations. The solid lines have the same value of $[\sim\mathrm{R}^\bullet]k_\mathrm{t}$ in each case, 0.1, and the height of each curve is proportional to $[\mathrm{M}]_0$. The model describes the data well, explaining the proportionality to monomer concentration and the ability of termination to stop the reaction at miniscule conversion levels.

For comparison, the $\mathrm{CuCl/CuCl_2/Me_6TREN}$ catalytic system was used to initiate the polymerization at room temperature. In the first attempts at using this catalyst,

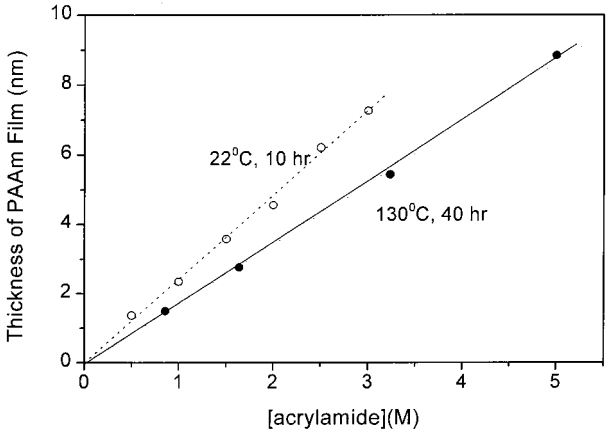


**Figure 2.** Thickness of polyacrylamide film vs acrylamide concentration for two different reaction temperatures: 22 and 130 °C. For a given termperture, [acrylamide] was the only component varied. The points are the experimental data, and the lines are from linear regressions.

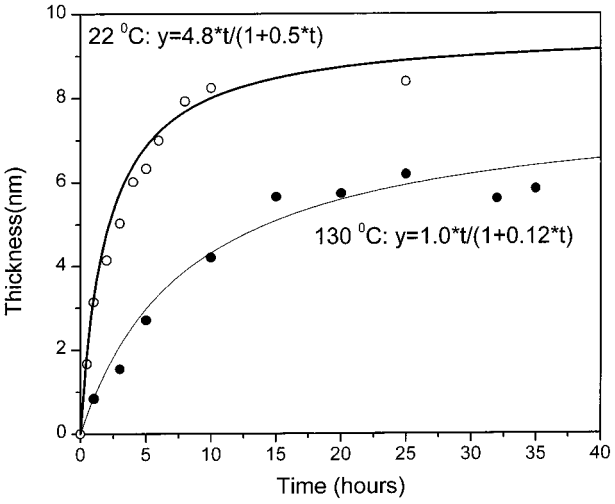


**Figure 3.** Thickness of polyacrylamide vs time for two different reaction temperatures: 22 and 130 °C. The points are the experimental data, and each of the curves represent the best fit to eq 5.

the same concentrations of Cu(I) and monomer concentrations, and the same solvent, were used as those that had been used for the 130 °C reaction. The reaction was uncontrolled, giving irreproducible results. We found that adding a large amount of Cu(II) was key to reproducible results. The results are reported here for a ratio of [Cu(I)]/[Cu(II)] = 10.

Figure 2 shows the polyacrylamide thickness as a function of monomer concentration for the room temperature polymerization on silicon wafers. On the same graph is shown the plot for the 130 °C polymerization for the same monomer concentration of 3 M. Despite the much higher amount of Cu(II) at room temperature, the slope of the line is actually higher at room temperature.

The kinetics of the chain growth were studied for the room-temperature polymerization, and the results are shown in Figure 3. The growth curves for polyacrylamide at the two temperatures are for the same monomer concentration. Both curves were fit to eq 9, as graphed by the solid curves. For the room-temperature case, the propagation rate, $[M]_0 k_p[\sim R^\bullet]_0$, is 5-fold faster than that of the high-temperature reaction (4.8/1.0), and the termination rate, $k_t[\sim R^\bullet]_0$, is also 5-fold faster (0.5/0.1). The result is that the final film is thicker at room temperature but is expected to be less uniform.

The model considers only radical combination as a means of termination. This can be tested by determining whether chlorine is lost at the surface. XPS measurements were performed, and the results are shown in Figure 4. For the benzyl chloride monolayer, the peak for chlorine is clearly visible, but for the 4 nm polyacrylamide film, the chlorine peak is hardly visible above the baseline. For the case of the 8 nm film, the chlorine peak is not visible. These results show that the chlorine atoms are less accessible to photoelectron spectroscopy, which is sensitive to the outer surface of the film. This could either be due to the chlorine atoms becoming inaccessible by being buried in the film or to loss of chlorine from termination reactions.

To investigate chlorine accessibility vs termination, the polyacrylamide film was prepared on silica gel to take advantage of the greater number of analytical techniques amenable to high surface area materials. Solid state $^{13}C$ NMR spectroscopy was used to probe mobility of the chains by line width, where a broader peak would indicate slower motion.[41] Cross-polarization and magic-angle spinning were used. Figure 5 shows the $^{13}C$ solid-state NMR spectra of silica gel samples for the benzyl chloride monolayer and for polyacrylamide film thickness prepared under conditions that gave 4 and 8 nm films on the silicon wafer. There is no obvious change in the width of the peak at 47 ppm, which corresponds to the two carbons of the acrylamide, indicating no significant change in mobility. Additionally, the resonance for the methylene group of the initiator drops as reaction proceeds, consistent with loss of chlorine.

The moles of chlorine can be tested directly though microanalysis of this higher surface area material as the reaction progresses. The calculations were simplified by first analyzing a sample of silica gel with only benzyl chloride and then using the remainder of this same material for polymerization so that the initial amount of benzyl chloride was known. For the silica gel with only benzyl chloride, the percent carbon is related to coverage of benzyl chloride directly.

$$\frac{\%\ C_{ini}}{100} = \frac{g_{bc}\frac{9\cdot 12}{FW_{bc}}}{g_{bc} + g_{SiO_2}} \qquad (10)$$

The grams of benzyl chloride and silica are indicated as $g_{bc}$ and $g_{SiO_2}$, respectively, and $FW_{bc}$ is the formula weight for the benzyl chloride reagent. Since the specific surface area of the bare silica is known, this allows moles/area to be calculated. The expression was solved for $g_{bc}/g_{SiO_2}$, and the known specific surface area of the silica, which was 100 $m^2/g$, was used to convert the result to moles per square meter. To test for self-consistency, the analogous expression for % Cl was also used to calculate molar coverage.

$$\frac{\%\ Cl_{ini}}{100} = \frac{g_{bc}\frac{35.5}{FW_{bc}}}{g_{bc} + g_{SiO_2}} \qquad (11)$$

Once polymerization proceeds, if termination occurs, chlorine is lost and the moles of benzyl groups are no longer coupled to the moles of chlorine, necessitating

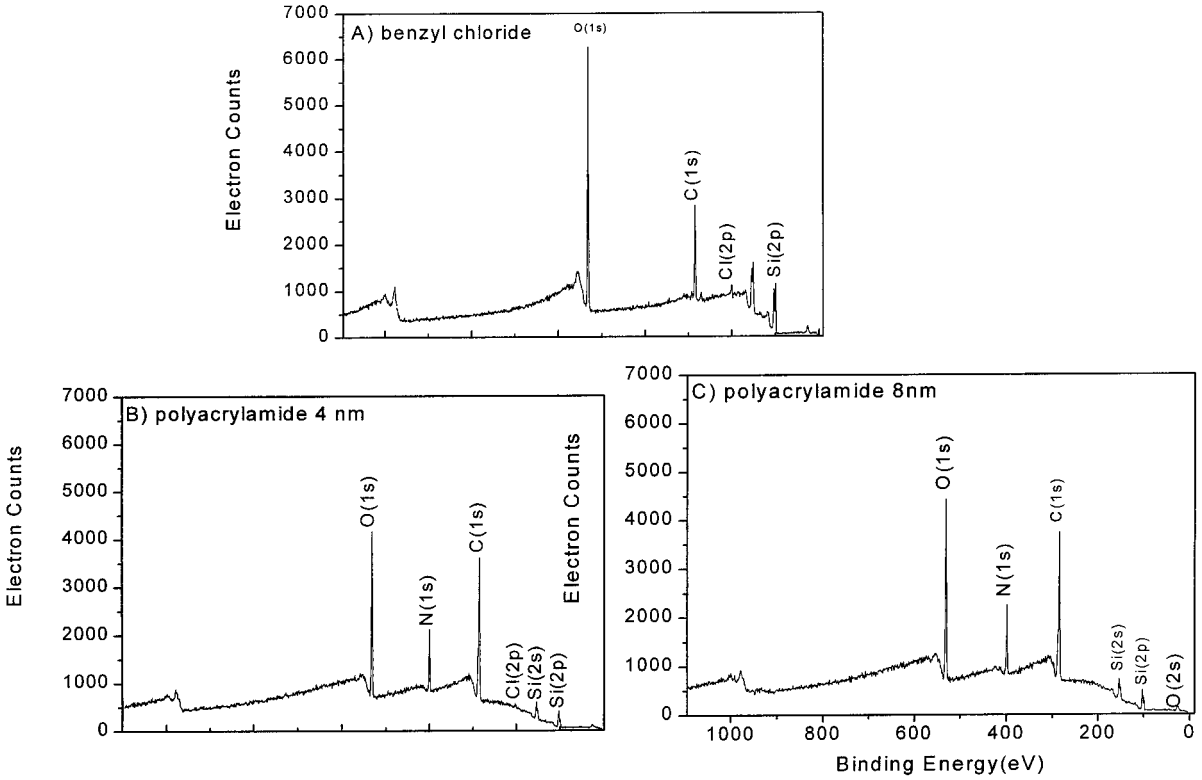


**Figure 4.** X-ray photoelectron spectra of films on silicon wafers: (A) benzyl chloride; (B) 4 nm polyacrylamide; (C) 8 nm polyacrylamide. The peak due to Cl is at 200 eV.

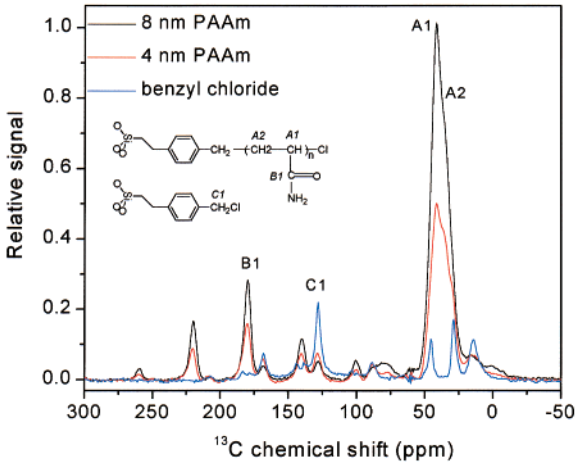


**Figure 5.** $^{13}$C NMR spectra, obtained with cross-polarization and magic angle spinning, for benzyl chloride (blue), 4 nm polyacrylamide (red), and 8 nm polyacrylamide (black). The resonances of interest are indicated with reference to the structures of acrylamide and benzyl chloride, shown in the figure.

more information in the microanalysis. Consequently, nitrogen microanalysis was done allowing the ratio to be used to determine $g_{AAm}/g_{SiO_2}$ and, hence, molar coverage of reacted acrylamide groups.

$$\frac{\%\ C}{\%\ N} = \frac{g_{bc}\frac{9\cdot 12}{FW_{bc}} + g_{AAm}\frac{3\cdot 12}{FW_{AAm}}}{g_{AAm}\frac{14}{FW_{AAm}}} \qquad (12)$$

Similarly, the ratio % Cl/% N allows determination of the molar coverage of chlorine atoms.

The results of the calculations from the microanalysis data are presented in Table 1. The carbon and chlorine analyses agreed within 3% for the initial coverage of benzyl chloride, which is shown to be a dense self-assembled monolayer of $7 \times 10^{-6}$ mol/m$^2$. Figure 6 shows a plot of the molar concentrations of acrylamide and chlorine on the surface as a function of time, where the solid lines simply connect the points. The mi-

**Table 1. Molar Coverages of the Initial Benzyl Chloride Monolayer (PhCl) before Polymerization and the Moles of Attached Acrylamide Units and Chlorine Atoms as a Function of Reaction Time, Each Calculated from Microanalysis Data, As Indicated**

| time, h | PhCl (mol/m$^2$) based on % C | PhCl (mol/m$^2$) based on % Cl | acrylamide (mol/m$^2$) based on % C | acrylamide (mol/m$^2$) based on % N | Cl (mol/m$^2$) based on % Cl |
|---|---|---|---|---|---|
| 0 | $7.1 \times 10^{-6}$ | $6.9 \times 10^{-6}$ | | | $6.9 \times 10^{-6}$ |
| 2 | | | $2.5 \times 10^{-5}$ | $2.3 \times 10^{-5}$ | $3.2 \times 10^{-6}$ |
| 10 | | | $3.8 \times 10^{-5}$ | $3.8 \times 10^{-5}$ | $2.3 \times 10^{-6}$ |
| 25 | | | $5.9 \times 10^{-5}$ | $5.8 \times 10^{-5}$ | $1.4 \times 10^{-6}$ |

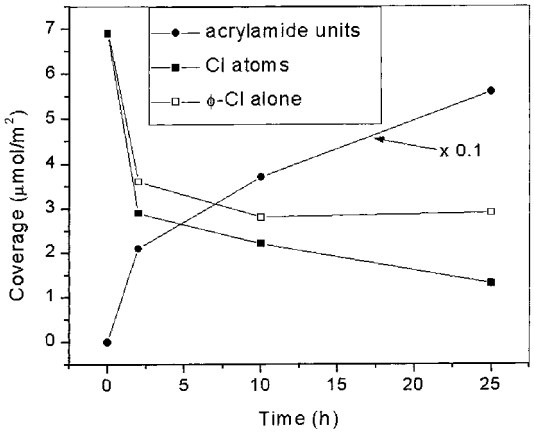


**Figure 6.** Plot of coverages vs time for chlorine (■) and acrylamide (●) for polymerization reaction and chlorine (○) in the absence of acrylamide monomer.

croanalysis results show that the chlorine coverage decreases rapidly very early in the reaction, then decreases much more slowly. The graph shows that coverage of acrylamide units jumps initially and then grows more slowly. The coverage of reacted acrylamide units is scaled by 10 to fit on the same graph as the chlorine coverage. The results confirm that termination is due to radical combination.

The shape of the kinetic curve for growth of acrylamide differs from that of the flat surface in that the curve for the silica gel does not level after 10 h. The surface area of silica gel is high enough that deviation from the model of eq 9 occurs: the ratio [Cu(I)]/[Cu(II)] is not constant over the course of the reaction. For the 0.5 g of silica gel used, and its specific area of 100 $m^2/g$, the 4 $\mu mol/m^2$ of chlorine atoms lost from the surface contribute to doubling the number of moles of Cu(II) in solution. The ratio [Cu(I)]/[Cu(II)] drops from 10 to 4.5, thereby lowering the radical concentration to slow termination. This persistent radical effect and Fisher's model become applicable once the surface area of the material is sufficiently high.

For the silica gel, one wonders whether only the benzyl chloride groups are involved in termination. This was answered by exposing benzyl chloride to the copper catalyst over the same reaction period, under the same reaction conditions but without acrylamide. The data, as graphed in Figure 6, show that benzyl chloride is responsible for most of the loss of chlorine. The loss of chlorine from benzyl chloride alone is almost complete in 2 h, and is complete at 5 h. The coverage of chlorine atoms drops from 7 to 3 $\mu mol/m^2$ and then is constant, rather than progressing to zero chlorine coverage. Second-order kinetics would predict the concentration would go to zero, but the leveling off to a constant can be explained by the benzyl chloride groups being immobilized; hence, they can only react with close neighbors and then the termination stops. When polymerization is occurring, the graph shows that the loss of chlorine continues after 2 h. This difference in behavior from benzyl chloride alone can be explained by the greater mobility of acrylamide chains than the benzyl groups. The resonance for the benzyl chloride group in the NMR spectrum of Figure 5 continues to drop through the reaction. It is possible that this late termination is due to reaction of benzyl radicals with acrylamide radicals.

The strategy of adding initiator into the solution is sometimes used to infer molecular weight and polydispersity of the tethered polymer chains on the surface. The idea is that the solution polymer lends itself more readily to analysis by gel permeation chromatography. The results here draw attention to the problem that the initiator concentration on the surface is potentially much higher, which would cause much greater termination on the surface.

## Conclusions

The results show that the polyacrylamide chains can be grown on silica surfaces at room temperature through atom-transfer radical polymerization using the CuCl/$CuCl_2$/$Me_6$TREN catalytic system. The results further show that polymer thickness can be controlled readily by monomer concentration. Finally, the results show that the polymerization under the present conditions is strongly affected by termination from radical combination, as demonstrated by the loss of chlorine from the surface. Radical combination is particularly a problem for surface polymerization because it is easy to prepare a surface for which the reactive groups are in close proximity. Since the propagation rate is linear in $[R^\bullet]$ but the termination rate is linear in $[R^\bullet]^2$, controlled growth of polymer from surfaces can be achieved by reducing the radical concentration.

**Acknowledgment.** This work was supported by the Department of Energy under contract DE-FG02-91ER-14187.

## References and Notes

(1) Wayland, B. B.; Poszmik, G.; Mukerjee, S. L.; Fryd, M. *J. Am. Chem. Soc.* **1994**, *116*, 7943−7944.
(2) Kato, M.; Kamigaito, M.; Sawamoto, M.; Higashimura. T. *Macromolecules* **1995**, *28*, 1721−1723.
(3) Percec, V.; Barboiu, B. *Macromolecules* **1995**, *28*, 7970−7972.
(4) Wang, J. S.; Matyjaszewski, K. *Macromolecules* **1995**, *28*, 7901−7910.
(5) Pattern, T. E.; Xia, J. H.; Abernathy, T.; Matyjaszewski, K. *Science* **1996**, *272*, 866.
(6) Prucker, O.; Rühe, J. *Langmuir* **1998**, *14*, 6893.
(7) Kelly, T. W.; Schorr, P. A.; Johnson, K. D.; Tirrell, M.; Frisbie, C. D. Direct *Macromolecules* **1998**, *31*, 4297.
(8) Koutsos, V.; van der, Vegte, E. W.; Hadziioannou, G. *Macromolecules* **1999**, *32*, 1233.
(9) Zhao, B.; Brittain, W. J. *Prog. Polym.* **2000**, *25*, 677.
(10) Husemann, M.; Mecerreyes, D.; Hawker, C. J.; Hedrick, J. L.; Shah, R.; Abbott, N. L. *Angew. Chem., Int. Ed.* **1999**, *38*, 647.
(11) Xia, J. H.; Matyjaszewski, K. *Macromolecules* **1997**, *30*, 7697.
(12) Pascual, S.; Coutin, B.; Tardi, M.; Polton, A.; Vairon, J.-P. *Macromolecules* **1999**, *32*, 1432.
(13) Matyjaszewski, K.; Wei, M. L.; Xia, J. H.; Gaynor, S. G. *Macromol. Chem. Phys.* **1998**, *199*, 2289.
(14) Matyjaszewski, K.; Patten, T. E.; Xia, J. H. *J. Am. Chem. Soc.* **1997**, *119*, 674.
(15) Percec, V.; Barboiu, B.; Kim, H.-J. *J. Am. Chem. Soc.* **1998**, *120*, 305.
(16) Mansky, P.; Liu, Y.; Huang, E.; Russell, T. P.; Hawker, C. *Science* **1997**, *275*, 1458.
(17) Hawker, C. J.; Malmström, E. E. *Macromol. Chem. Phys.* **1998**, *199*, 923.
(18) Hawker, C. J.; Barclay, G. G.; Dao, J. *J. Am. Chem. Soc.* **1996**, *118*, 11467.
(19) de Boer, B.; Simon, H. K.; Werts, M. P. L.; van de Vegte, E. W.; Hadziioannou, G. *Macromolecules* **2000**, *33*, 349.
(20) Sedjo, R. A.; Mirous, B. K.; Britain, W. J. *Macromolecules* **2000**, *33*, 1492.
(21) Matyjaszewski, K.; Miller, P. J.; Shukla, N.; Immaraporn, B.; Gelman, A.; Luokala, B. B.; Siclovan, T. M.; Kickelbick, G.; Vallant, T.; Hoffmann, H.; Pakula, T. *Macromolecules* **1999**, *32*, 8716.
(22) Husseman, M.; Malmström, E. E.; McNamara, M.; Mate, M.; Mecerreyes, D.; Benoit, D. G.; Hedrick, J. L.; Mansky, P.; Huang, E.; Russell, T. P.; Hawker, C. J. *Macromolecules* **1999**, *32*, 1424.
(23) Huang, X. Y.; Wirth, M. J. *Anal. Chem.* **1997**, *69*, 4577.
(24) Huang, X. Y.; Doneski, L. J.; Wirth, M. J. *Anal. Chem.* **1998**, *70*, 4023.
(25) Wirth, M. J.; Huang, X. *Macromolecules* **1999**, *32*, 1694.
(26) Ejaz, M.; Yamamoto, S.; Ohno, K.; Tsujii, Y.; Fukuda, T. *Macromolecules* **1998**, *31*, 5934.
(27) Hawker, C. J.; Mecerreyes, D.; Elce, E.; Dao, J.; Hedrick, J. L.; Barakat, I.; Dubrois, P.; Jérôme, R.; Volksen, W. *Macromol. Chem. Phys.*. **1997**, *198*, 155.
(28) Matyjaszewski, K.; Shipp, D. A.; Wang, J. L.; Grimaud, T.; Pattern, T. E. *Macromolecules* **1998**, *31*, 6836.
(29) Percec, V.; Barboiu, B.; Neumann, A.; Ronda, J. C.; Zhao, M. *Macromolecules* **1996**, *29*, 3665.
(30) Ohno, K.; Fujimoto, K.; Tsujii, Y, Fukuda, T. *Polymer* **1999**, *40*, 759.
(31) Percec, V.; Barboiu, B. *Macromolecules* **1995**, *28*, 7970.
(32) Nishikawa, T.; Ando, T.; Kamigaito, M.; Sawamoto, M. *Macromolecules* **1997**, *30*, 2244.
(33) Liou, S.; Rademacher, J. T.; Malaba, D.; Pallack, M. E.; Brittain, W. J. *Macromolecules* **2000**, *33*, 4295.
(34) Hovestad, N. J.; van Koten, G.; Bon, S. A. F.; Haddleton, D. M. *Macromolecules* **1998**, *31*, 7999.

(35) Kajiwara, A.; Matyjaszewski, K. *Polym. J.* **1999**, *31*, 70.
(36) Woodworth, B. E.; Metzner, Z.; M.; Matyjaszewski, K. *Macromolecules* **1998**, *31*, 7999.
(37) Beers, K. L.; Gaynor, S. G.; Matyjaszewski, K. *Macromolecules* **1998**, *31*, 9413.
(38) Shipp, D. A.; Wang, J. L.; Matyjaszewski, K. *Macromolecules* **1998**, *31*, 8005.
(39) Grubbs, R. B.; Hawker, C. J.; Dao, J.; Fréchet, J. M. J. *Angew. Chem., Int. Ed. Engl.* **1997**, *36*, 270.
(40) Teodorescu, M.; Matyjaszewski, K. *Macromolecules* **1999**, *32*, 4826.
(41) Teodorescu, M.; Matyjaszewski, K. *Macromol. Rapid Commun.* **2000**, *21*, 190.
(42) Ehsan, M. Q.; Ohba, Y.; Yamauchi, S.; Iwaizumi, M. *Bull. Chem. Soc. Jpn.* **1996**, *69*, 2201.
(43) Huang, X. Y. Surface-confined Living Radical Polymerization for Improvement of Biological Molecule Separation. Doctoral Thesis, University of Delaware, 1998.
(44) Matyjaszewski, K.; Davis, K.; Pattern, T. E.; Wei, M. *Tetrahedron* **1997**, *53*, 15321.
(45) Ciampolini, M.; Nardi, N. *Inorg. Chem.* **1966**, *5*, 41.
(46) Zeigler, R. C.; Maciel, G. E. *J. Phys. Chem.* **1991**, *95*, 7345.
(47) Swinton, D. J.; Wirth, M. J. *Anal. Chem.* **2000**, *72*, 3725.
(48) Fischer, H. *J. Polym. Sci., Part A* **1999**, *37*, 1885−1901.

MA011313X